Kellie V. Stoka
Department of Mechanical Engineering
and Materials Science,
Washington University,
St. Louis, MO 63130

Justine A. Maedeker
Department of Mechanical Engineering
and Materials Science,
Washington University,
St. Louis, MO 63130

Lisa Bennett
Department of Biomedical Engineering,
Saint Louis University,
St. Louis, MO 63130

Siddharth A. Bhayani
Department of Biomedical Engineering,
Saint Louis University,
St. Louis, MO 63130

William S. Gardner
Department of Biomedical Engineering,
Saint Louis University,
St. Louis, MO 63130

Jesse D. Procknow
Department of Mechanical Engineering
and Materials Science,
Washington University,
St. Louis, MO 63130

Austin J. Cocciolone
Department of Mechanical Engineering
and Materials Science,
Washington University,
One Brookings Dr., CB 1185,
St. Louis, MO 63130

Tezin A. Walji
Department of Cell Biology and Physiology,
Washington University,
St. Louis, MO 63130

Clarissa S. Craft
Department of Cell Biology and Physiology,
Washington University,
St. Louis, MO 63130

Jessica E. Wagenseil[1]
Department of Mechanical Engineering
and Materials Science,
Washington University,
One Brookings Dr., CB 1185,
St. Louis, MO 63130
e-mail: jessica.wagenseil@wustl.edu

Effects of Increased Arterial Stiffness on Atherosclerotic Plaque Amounts

Increased arterial stiffness is associated with atherosclerosis in humans, but there have been limited animal studies investigating the relationship between these factors. We bred elastin wildtype ($Eln^{+/+}$) and heterozygous ($Eln^{+/-}$) mice to apolipoprotein E wildtype ($Apoe^{+/+}$) and knockout ($Apoe^{-/-}$) mice and fed them normal diet (ND) or Western diet (WD) for 12 weeks. $Eln^{+/-}$ mice have increased arterial stiffness. $Apoe^{-/-}$ mice develop atherosclerosis on ND that is accelerated by WD. It has been reported that $Apoe^{-/-}$ mice have increased arterial stiffness and that the increased stiffness may play a role in atherosclerotic plaque progression. We found that $Eln^{+/+}Apoe^{-/-}$ arterial stiffness is similar to $Eln^{+/+}Apoe^{+/+}$ mice at physiologic pressures, suggesting that changes in stiffness do not play a role in atherosclerotic plaque progression in $Apoe^{-/-}$ mice. We found that $Eln^{+/-}Apoe^{-/-}$ mice have increased structural arterial stiffness compared to $Eln^{+/+}Apoe^{-/-}$ mice, but they only have increased amounts of ascending aortic plaque on ND, not WD. The results suggest a change in atherosclerosis progression but not end stage disease in $Eln^{+/-}Apoe^{-/-}$ mice due to increased arterial stiffness. Possible contributing factors include increased blood pressure and changes in circulating levels of interleukin-6 (IL6) and transforming growth factor beta 1 (TGF-β1) that are also associated with $Eln^{+/-}$ genotype. [DOI: 10.1115/1.4039175]

Keywords: elastin, atherosclerosis, compliance, vascular mechanics

Introduction

Increased arterial stiffness is a risk factor for atherosclerosis. Increased arterial stiffness, as measured by pulse wave velocity (PWV), is associated with coronary artery disease, peripheral artery disease, and atherosclerotic vascular damage [1]. PWV is related to the material stiffness of the vascular wall, as well as the

[1]Corresponding author.
Manuscript received October 27, 2017; final manuscript received January 4, 2018; published online March 5, 2018. Assoc. Editor: Raffaella De Vita.

internal radius and wall thickness, hence it is a measure of structural stiffness [2]. Increased PWV changes the interaction of reflected waves within the circulatory system leading to alterations in shear stress patterns. Prolonged oscillatory shear stress induces endothelial cell expression of adhesion and inflammatory molecules [3]. Altered structural stiffness can affect the mechanical stress and stretch experienced by vascular wall cells. Cellular responses to different levels of cyclic stretch include production of reactive oxygen species, kinase and transcription factor activation, cytoskeletal changes, and enhanced metabolism [4]. In vitro, smooth muscle cell phenotype depends on the material stiffness of the underlying substrate [5]. Changes in cellular phenotype and signaling likely converge and contribute to changes in atherosclerosis susceptibility associated with increased arterial stiffness.

Apolipoprotein E knockout ($Apoe^{-/-}$) mice develop spontaneous atherosclerosis on normal diet (ND) [6] that is accelerated with Western diet (WD) [7] and are the most extensively studied animal model of atherosclerosis. Agianniotis and Stergiopulos [8] demonstrated increased structural and material stiffness of contracted and relaxed $Apoe^{-/-}$ thoracic aorta in vitro for 10–12-week-old mice on ND. However, Cilla et al. [9] showed no differences in passive structural or material stiffness of the entire aorta in situ for $Apoe^{-/-}$ compared to $Apoe^{+/+}$ mice on ND for 10–40 weeks. Differences between the two studies could be due to differences in arterial segments investigated, in vitro versus in situ methods, or smooth muscle activation state. The first goal of our study is to quantify passive structural and material arterial stiffness in $Apoe^{-/-}$ and $Apoe^{+/+}$ mice on ND and WD to determine if a predisposition to increased stiffness may play a role in atherosclerotic lesion formation. We chose to examine left common carotid arteries, as they are amenable to in vitro pressure-diameter studies and do not develop extensive plaques at the early stages of atherosclerotic disease in $Apoe^{-/-}$ mice [10], so mechanical measurements are not confounded by the stiffness of plaques attached to the arterial wall.

Arterial stiffness in mice can be altered by genetic modification of extracellular matrix components. Elastin haploinsufficient ($Eln^{+/-}$) mice have reduced elastin amounts and increased structural arterial stiffness [11,12]. Elastic lamellae in the $Eln^{+/-}$ arterial wall are thinner than $Eln^{+/+}$, but are not fragmented or degraded [13]. The second goal of our study is to significantly increase arterial stiffness of $Apoe^{-/-}$ mice by crossing them with $Eln^{+/-}$ mice and quantify atherosclerotic plaque amounts to investigate the role of arterial stiffness in atherosclerotic disease. We put $Eln^{+/+}Apoe^{+/+}$, $Eln^{+/+}Apoe^{-/-}$, $Eln^{+/-}Apoe^{+/+}$, and $Eln^{+/-}Apoe^{-/-}$ mice on ND or WD for 12 weeks and performed in vitro pressure-diameter tests on the carotid artery to determine structural and material stiffnesses. We quantified aortic valve and ascending aorta plaque amounts, serum cholesterol, blood pressure, and examined arterial wall structure. For the $Apoe^{-/-}$ group, we also measured serum cytokine levels. Our results suggest that arterial stiffness is not altered by the lack of *Apoe* expression and that increased structural stiffness due to elastin haploinsufficiency, in addition to contributing factors such as hypertension and altered levels of circulating cytokines, may alter the progression of atherosclerotic plaque accumulation.

Materials and Methods

Mice. $Apoe^{-/-}$ mice were purchased from The Jackson Laboratory (#002052, Bar Harbor, ME) and bred with $Eln^{+/-}$ mice [14]. Siblings were mated to obtain male $Eln^{+/+}Apoe^{+/+}$, $Eln^{+/+}Apoe^{-/-}$, $Eln^{+/-}Apoe^{+/+}$, and $Eln^{+/-}Apoe^{-/-}$ mice. Males were used for comparison to the previous studies on $Eln^{+/-}$ [11,12] and $Eln^{+/-}Ldlr^{-/-}$ (low density lipoprotein (LDL) receptor) mice [13] and to eliminate sex as an independent variable. All mice with $Eln^{-/-}$ genotype die at birth and were not included in the study [14]. Mice were weaned at three weeks of age, provided with ND (5% fat, 0% cholesterol) or WD (20% fat, 0.15% cholesterol) from TestDiet (AIN-76A, St. Louis, MO) for 12 weeks, and then sacrificed. A total of 97 mice were used for the study. All protocols were approved by the Institutional Animal Care and Use Committee.

Blood Pressure, Blood Chemistry, and Tissue Collection. Mice were anesthetized with 2% isoflurane and arterial blood pressure was measured with a solid-state catheter (Transonic, Ithaca, NY). Whole blood was collected by cardiac puncture. Serum was separated and stored at −80 °C until analyzed for lipid levels by Advanced Veterinary Laboratory (St. Louis, MO) or for cytokine levels by the Immunomonitoring Laboratory at Washington University (St. Louis, MO). Levels of inflammatory proteins (V-PLEX Proinflammatory Panel 1, mouse) and transforming growth factor beta 1 (TGF-β1) (Human, cross-reacts with mouse) were measured using electrochemiluminescence immunoassays (Mesoscale Discovery, Rockville, MD). The numbers of animals in each group for blood pressure and serum measurements are listed in Tables 1–3. The proximal section of the heart was removed and frozen at −80 °C in Tissue Tek OCT for sectioning of the aortic root ($N = 9$ $Eln^{+/+}Apoe^{-/-}$ ND, 8 $Eln^{+/+}Apoe^{-/-}$ WD; 9 $Eln^{+/-}Apoe^{-/-}$ ND; 8 $Eln^{+/-}Apoe^{-/-}$ WD; 9 $Eln^{+/+}Apoe^{+/+}$ ND; 9 $Eln^{+/+}Apoe^{+/+}$ WD; 9 $Eln^{+/-}Apoe^{+/+}$ ND; and 6 $Eln^{+/-}Apoe^{+/+}$ WD). The entire aorta from the base to the iliac bifurcation was removed and fixed for en face plaque analysis ($N = 8$ $Eln^{+/+}Apoe^{-/-}$ ND, 8 $Eln^{+/+}Apoe^{-/-}$ WD;

Table 1 Blood pressure was measured under anesthesia using a solid-state catheter. $Eln^{+/-}$ mice have increased systolic and pulse pressures. *P* values are from three-way ANOVA for diet, *Apoe* genotype, *Eln* genotype, and all interactions between independent variables. Only significant interactions are listed. Significant *p* values (< 0.05) are shown in italics. *N* is the number of animals in each group.

			Blood pressure (mmHg)				
Diet	Apoe	Eln	Sys	Dias	Pulse	HR (bpm)	N
ND	$Apoe^{+/+}$	$Eln^{+/+}$	113±11	78±7	34±5	553±46	10
		$Eln^{+/-}$	119±10	76±7	43±8	527±38	11
	$Apoe^{-/-}$	$Eln^{+/+}$	106±6	75±4	33±3	535±45	10
		$Eln^{+/-}$	127±11	83±8	45±7	521±34	10
WD	$Apoe^{+/+}$	$Eln^{+/+}$	116±7	79±5	35±4	550±46	12
		$Eln^{+/-}$	123±13	78±7	46±10	514±55	10
	$Apoe^{-/-}$	$Eln^{+/+}$	123±11	87±11	36±3	524±64	10
		$Eln^{+/-}$	124±13	78±10	45±9	463±53	11
P value		diet	*0.035*	0.137	0.169	*0.044*	
		Apoe	0.256	0.091	0.974	*0.019*	
		Eln	*< .001*	0.448	*<.001*	*0.002*	
		interactions	Eln x Diet (*.045*)	Eln x Diet (*.017*)			

Table 2 Cholesterol levels were measured from serum samples. *Apoe*$^{-/-}$ mice on WD have increased total cholesterol, increased LDL, decreased HDL, and no changes in triglycerides (tri). *P* values are from three-way ANOVA for diet, *Apoe* genotype, *Eln* genotype, and all interactions between independent variables. Only significant interactions are listed. Significant *p* values (< 0.05) are shown in italics. *N* is the number of animals in each group.

			Serum cholesterol (mg/dl)				
Diet	*Apoe*	*Eln*	Total	Tri	LDL	HDL	N
ND	*Apoe*$^{+/+}$	*Eln*$^{+/+}$	132±14	66±10	7±1	71±6	6
		Eln$^{+/-}$	125±27	61±12	5±2	69±13	8
	Apoe$^{-/-}$	*Eln*$^{+/+}$	780±165	225±94	67±32	47±12	8
		Eln$^{+/-}$	710±134	179±68	63±27	41±13	7
WD	*Apoe*$^{+/+}$	*Eln*$^{+/+}$	206±77	73±18	11±4	104±18	7
		Eln$^{+/-}$	166±50	69±14	10±3	99±26	7
	Apoe$^{-/-}$	*Eln*$^{+/+}$	1122±60	216±75	641±293	20±6	8
		Eln$^{+/-}$	1088±126	254±133	422±162	27±15	7
P value		diet	*< .001*	0.301	*<.001*	0.317	
		Apoe	*< .001*	*< .001*	*< .001*	*< .001*	
		Eln	0.177	0.834	0.091	0.933	
		interactions	Apoe x Diet (< .001)		Apoe x Diet (< .001)	Apoe x Diet (< .001)	

8 *Eln*$^{+/-}$*Apoe*$^{-/-}$ ND; 7 *Eln*$^{+/-}$*Apoe*$^{-/-}$ WD; 4 *Eln*$^{+/+}$*Apoe*$^{+/+}$ ND, 5 *Eln*$^{+/+}$*Apoe*$^{+/+}$ WD; 4 *Eln*$^{+/-}$*Apoe*$^{+/+}$ ND; and 4 *Eln*$^{+/-}$*Apoe*$^{+/+}$ WD). The left common carotid artery was removed and stored at 4 °C for up to three days in physiologic saline before mechanical testing [15] (*N* = 8 *Eln*$^{+/+}$*Apoe*$^{-/-}$ ND, 7 *Eln*$^{+/+}$*Apoe*$^{-/-}$ WD; 5 *Eln*$^{+/-}$*Apoe*$^{-/-}$ ND; 7 *Eln*$^{+/-}$*Apoe*$^{-/-}$ WD; 6 *Eln*$^{+/+}$*Apoe*$^{+/+}$ ND, 7 *Eln*$^{+/+}$*Apoe*$^{+/+}$ WD; 6 *Eln*$^{+/-}$*Apoe*$^{+/+}$ ND; and 6 *Eln*$^{+/-}$*Apoe*$^{+/+}$ WD).

Mechanical Testing. Before removing the heart or any arteries, the mouse was placed in the supine position with the head tilted back for access to the carotid arteries in the neck. Small particles of activated charcoal were placed on the superior and inferior end of the left common carotid artery. Images were taken before and after dissection, and the in vivo axial stretch was determined by comparing the centerline distance between particles at each end of the artery. Some *Eln*$^{+/-}$*Apoe*$^{+/+}$ and *Eln*$^{+/-}$*Apoe*$^{-/-}$ carotid arteries were tortuous upon removal [12]. For tortuous arteries, we attempted to keep the artery in a single plane during imaging and the centerline of the artery was traced along the tortuous path for length measurements. The carotid artery was then mounted at its in vivo axial stretch ratio in a pressure myograph (110P, DMT-USA, Ann Arbor, MI) in physiologic saline solution at 37 °C. Arteries were inflated from 0 to 175 mmHg in steps of 25 mmHg (12 s/step), while pressure (P) and loaded outer diameter (d_o) were recorded at 1 Hz [12].

Histology. After mechanical testing, the carotid artery was fixed in 10% neutral buffered formalin overnight, dehydrated in a graded series of ethanol, embedded in paraffin, sectioned, stained with hematoxylin and eosin (H&E), Verhoeff Van Gieson (VVG), or picrosirius red (PSR), and imaged. Outer and inner wall boundaries of the unloaded artery sections were traced on H&E images (Fig. 2(*a*)) and fitted with ellipses using IMAGE J software (NIH, Bethesda, MD). The equivalent circular outer (D_o) and inner diameters (D_i) were determined assuming a constant area. Measured unloaded dimensions were scaled by 110% to account for shrinkage during histological processing [16].

Data Analyses. The loaded inner diameter of the carotid artery (d_i) was calculated from the loaded outer diameter, axial stretch ratio, and the unloaded dimensions by incompressibility. The average circumferential stretch (λ_θ) was calculated by

$$\lambda_\theta = \frac{d_i + d_o}{D_i + D_o} \tag{1}$$

The average circumferential Cauchy stress (σ_θ) was calculated by [17]

$$\sigma_\theta = \frac{P d_i}{d_o - d_i} \tag{2}$$

To determine the outer diameter for any applied pressure, the pressure-outer diameter data for one loading cycle were fit to Ref. [18]

$$d_o = a_1 + a_2\left\{1 - \exp\left(-\frac{P^{a_3}}{a_4}\right)\right\} \tag{3}$$

Table 3 Levels of inflammatory cytokines and TGF-β1 were measured from serum samples in *Apoe*$^{-/-}$ mice. WD increases levels of IL6, CXCL1, and TNF. *Eln*$^{+/-}$ mice have increased levels of IL6 and decreased levels of TGF-β1. *P* values are from two-way ANOVA for diet, *Eln* genotype, and the interaction between diet and *Eln* genotype. Significant *p* values (< 0.05) are shown in italics. *N* is the number of animals in each group.

		Inflammatory cytokines (pg/ml)						
Diet	Genotype	IL6	IL10	CXCL1	TNF	N	TGF-β1 (ng/ml)	N
ND	*Eln*$^{+/+}$*Apoe*$^{-/-}$	37±31	17±4	72±34	14±8	7	76±30	6
	Eln$^{+/-}$*Apoe*$^{-/-}$	65±39	23±24	54±14	11±2	5	47±15	5
WD	*Eln*$^{+/+}$*Apoe*$^{-/-}$	67±58	25±4	283±214	25±8	6	54±11	7
	Eln$^{+/-}$*Apoe*$^{-/-}$	158±106	20±9	210±127	28±12	4	40±16	4
P value	Diet	*0.03*	0.64	*0.006*	*< 0.001*		0.115	
	Eln	*0.034*	0.891	0.451	0.934		*0.022*	
	interactions	0.244	0.35	0.649	0.386		0.372	

where a_i are constants determined by regression using MATLAB software (Mathworks, Natick, MA). The mean R^2 for Eq. (3) fitted to the experimental data was 0.95±0.01. To compare physiologic values of different metrics, the measured blood pressures for each animal were used along with the mechanical testing data to calculate the systolic circumferential stress and stretch ratio, Peterson's modulus (E_p), and incremental Young's modulus (E_{inc}). Peterson's modulus is a measure of structural stiffness that is often used clinically [2]

$$E_P = \frac{d_{i,\text{dias}}(P_{\text{sys}} - P_{\text{dias}})}{d_{i,\text{sys}} - d_{i,\text{dias}}} \tag{4}$$

The incremental Young's modulus is a measure of material stiffness that linearizes the stress–strain curve in the physiologic pressure range [2]

$$E_{\text{inc}} = \frac{d_{i,\text{dias}} d_{i,\text{sys}}(P_{\text{sys}} - P_{\text{dias}})}{(d_{o,\text{sys}} - d_{i,\text{sys}})(d_{i,\text{sys}} - d_{i,\text{dias}})} \tag{5}$$

Plaque Quantification. For plaque quantification at the aortic valve, frozen sections of the aortic root were stained with oil red O in 60% isopropanol [19]. Images were taken of sections at approximately 10 μm intervals. For each mouse, three images with clear sections of the aortic valves were analyzed for total oil red O positive pixels using MATLAB software and averaged. For en face plaque quantification, the entire aorta was fixed in 10% neutral buffered formalin overnight, stored in phosphate buffered saline at 4 °C, then cut longitudinally and pinned to black wax in a petri dish [20]. The aorta was stained with oil red O in propylene glycol and imaged. As most of the plaque accumulates in the ascending aorta after 12 weeks on WD [9], only plaque in the ascending aortic region was quantified. The edges and positive oil red O pixels in the ascending aorta were manually traced using IMAGE J software. Plaque area was calculated as a percentage of positive oil red O pixels over the ascending aortic surface area.

Statistics. The Shapiro Wilk test [21] was used to determine if the data were normally distributed. All data passed the normality test except for pulse pressure for $Eln^{+/+}Apoe^{+/+}$ ND and $Eln^{+/-}Apoe^{+/+}$ WD, heart rate for $Eln^{+/-}Apoe^{-/-}$ WD, and circumferential stretch ratio for $Eln^{+/+}Apoe^{-/-}$ ND. As there was not one specific group or measurement that violated the normality assumption and analysis of variance (ANOVA) is relatively robust to violations of normality [22], ANOVA was used to test for statistical differences for all data. Three-way ANOVA was used to determine the effects of diet, *Apoe* genotype, *Eln* genotype, and their interactions. Two-way ANOVA was used to determine the effects of diet and *Eln* genotype and their interactions for serum cytokine levels in $Apoe^{-/-}$ mice. As *Eln* genotype was the main focus of the study, one-way ANOVA with Sidaks's test for multiple comparisons was used to investigate differences between *Eln* genotypes for specific groups (i.e., $Eln^{+/+}Apoe^{-/-}$ WD versus $Eln^{+/-}$ $Apoe^{-/-}$ WD). $P < 0.05$ was considered significant. All statistical analyses were performed using SPSS Statistics (IBM, Armonk, NY) or Prism (Graphpad, La Jolla, CA).

Results

$Eln^{+/-}$ Carotid Arteries Have Altered Pressure-Diameter Behavior and Reduced Axial Stretch. The in vivo axial stretch ratio of the carotid arteries was measured by comparing lengths before and after dissection. Overall, $Eln^{+/-}$ arteries have 19% smaller in vivo axial stretch ratios than $Eln^{+/+}$ ($p < 0.001$). *Apoe* genotype and diet have no effect on the in vivo axial stretch ratio and there are no interactions between independent variables. By one-way ANOVA, there are significant differences between $Eln^{+/-}$ and $Eln^{+/+}$ arteries for each group (Fig. 1(*a*)). Carotid arteries were mounted in the pressure myograph at the measured in vivo axial stretch ratio and pressurized from 0–175 mmHg. Overall, $Eln^{+/-}$ arteries have 6–11% smaller diameters than $Eln^{+/+}$ at all pressures ($p = < 0.001$–0.003). $Apoe^{-/-}$ arteries are 4% smaller than $Apoe^{+/+}$ at 75 mmHg only ($p = 0.03$) (Figs. 1(*b*) and 1(*c*)). Diet has no effect on arterial diameter and there are no interactions between independent variables. These results show that *Eln* genotype alters arterial pressure-diameter diameter behavior, while *Apoe* genotype has minimal effects. The pressure-diameter behavior is related to the structural stiffness of the arterial wall.

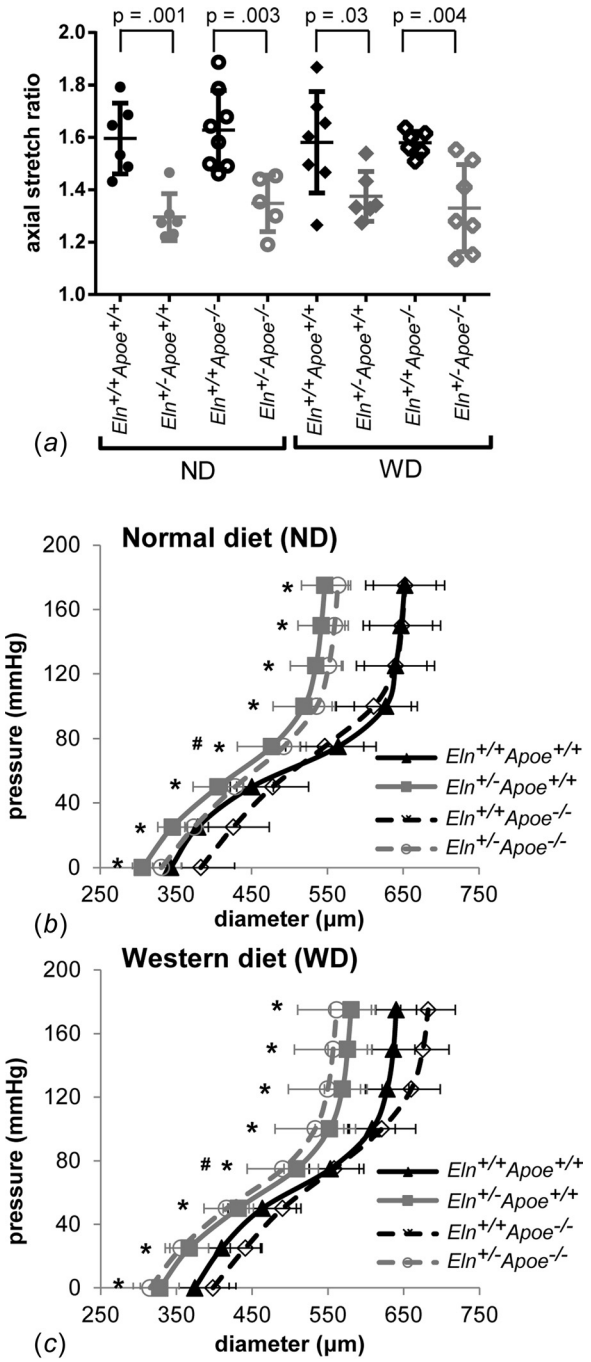

Fig. 1 In vivo axial stretch ratios (*a*) were measured by imaging the carotid artery before and after dissection. Individual measurements are shown with mean±SD. *P* values are from one-way ANOVA for *Eln* genotype. Mean carotid artery pressure-diameter curves from in vitro mechanical tests are shown for mice on ND (*b*) or WD (*c*) for 12 weeks after weaning. Significant effect of **Eln* genotype or #*Apoe* genotype by three-way ANOVA.

Carotid Artery Circumferential Cauchy Stress-Stretch Behavior is Similar Across Groups. Images of H&E stained sections were analyzed to determine the unloaded diameter and thickness of each carotid artery (Fig. 2(*a*)). On average, $Eln^{+/-}$ arteries have 10% smaller unloaded diameters than $Eln^{+/+}$ ($p < 0.001$). *Apoe* genotype and diet have no effect on the unloaded diameter and there are no interactions between independent variables. By one-way ANOVA, there are significant differences between $Eln^{+/-}Apoe^{-/-}$ WD and $Eln^{+/+}Apoe^{-/-}$ WD unloaded diameters (Fig. 2(*b*)). *Eln* genotype, *Apoe* genotype, and diet have no significant effects on unloaded thickness; however, there is a significant interaction between *Eln* genotype and diet ($p = 0.005$). By one-way ANOVA, there are significant differences in unloaded wall thicknesses between $Eln^{+/-}Apoe^{+/+}$ ND and $Eln^{+/+}Apoe^{+/+}$ ND arteries (Fig. 2(*c*)). The unloaded dimensions and pressure-diameter behavior were used to calculate the circumferential Cauchy stress-stretch behavior, which is similar across groups (Fig. 3). Therefore, changes in loaded pressure-diameter behavior are balanced by changes in unloaded dimensions for $Eln^{+/-}$ arteries to provide circumferential Cauchy stress-stretch behavior similar to $Eln^{+/+}$ arteries. We find no changes in circumferential Cauchy stress-stretch behavior of the carotid artery due to *Apoe* genotype or diet. The circumferential Cauchy stress-stretch behavior is related to the material stiffness of the arterial wall.

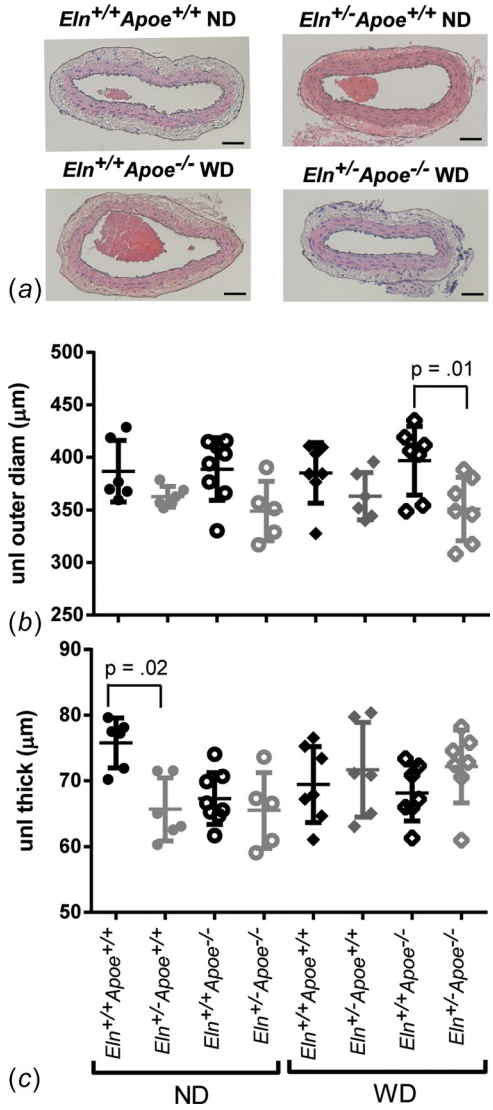

Fig. 2 Inner and outer carotid artery boundaries were traced on images of H&E stained sections to obtain unloaded dimensions. Representative sections for four of the eight groups are shown in (*a*). Scale bars = 50 μm. $Eln^{+/-}$ arteries have smaller unloaded diameters (*b*) and thicknesses (*c*). *P* values are from one-way ANOVA for *Eln* genotype. Results for three-way ANOVA are given in the text. Individual measurements are shown with mean±SD.

$Eln^{+/-}$ Mice Have Systolic Hypertension and Increased Carotid Artery Structural Stiffness. To determine the physiologic pressure range for each group, we measured arterial pressures under anesthesia using a solid-state catheter. On average, $Eln^{+/-}$ genotype increases systolic and pulse pressures, 8 and 30%, respectively, compared to $Eln^{+/+}$ (Table 1). *Apoe* genotype has no effect on blood pressure. WD increases systolic blood pressure 4%. There are interactions between *Eln* genotype and diet for systolic and diastolic blood pressures. *Eln* genotype, *Apoe* genotype, and WD all decrease heart rate 4–5%. These results indicate that *Eln* genotype is associated with isolated systolic hypertension and increased pulse pressure.

Using the measured blood pressures for each mouse, we determined the circumferential stress and stretch at systolic pressure and the structural (E_p) and material (E_{inc}) stiffnesses in the diastolic–systolic pressure range (Fig. 4). Overall, $Eln^{+/-}$ carotid arteries have 28% smaller systolic circumferential Cauchy stresses ($p = 0.001$) and 29% larger E_p ($p = 0.014$) than $Eln^{+/+}$, with no significant differences in systolic circumferential stretch or E_{inc}. *Apoe* genotype and diet have no effects on systolic circumferential

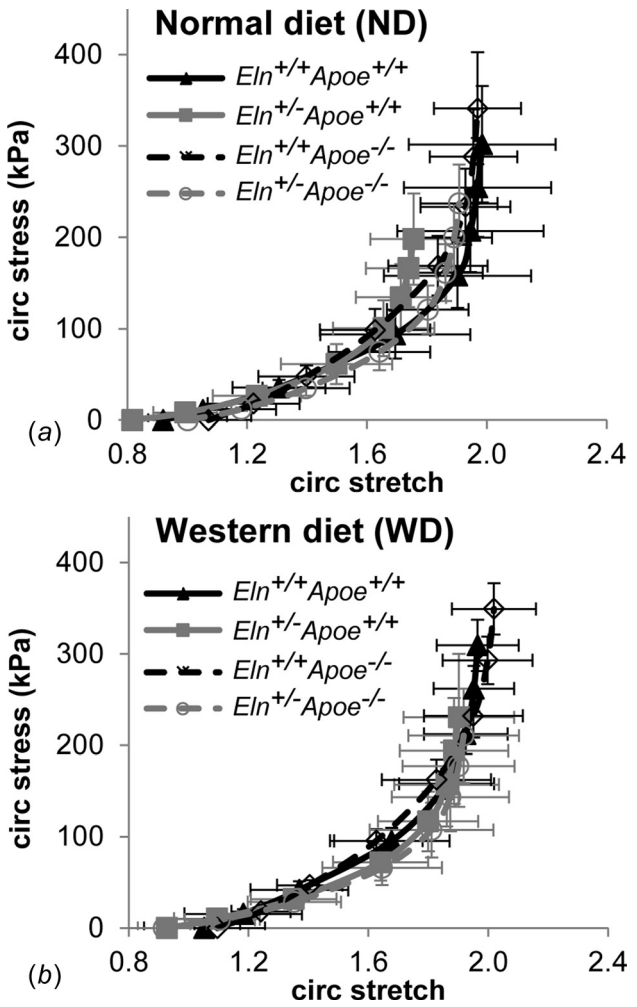

Fig. 3 Circumferential Cauchy stress-stretch relationships for the carotid arteries were calculated from the pressure-diameter behavior and the unloaded dimensions for each group on ND (*a*) and WD (*b*). Mean±SD.

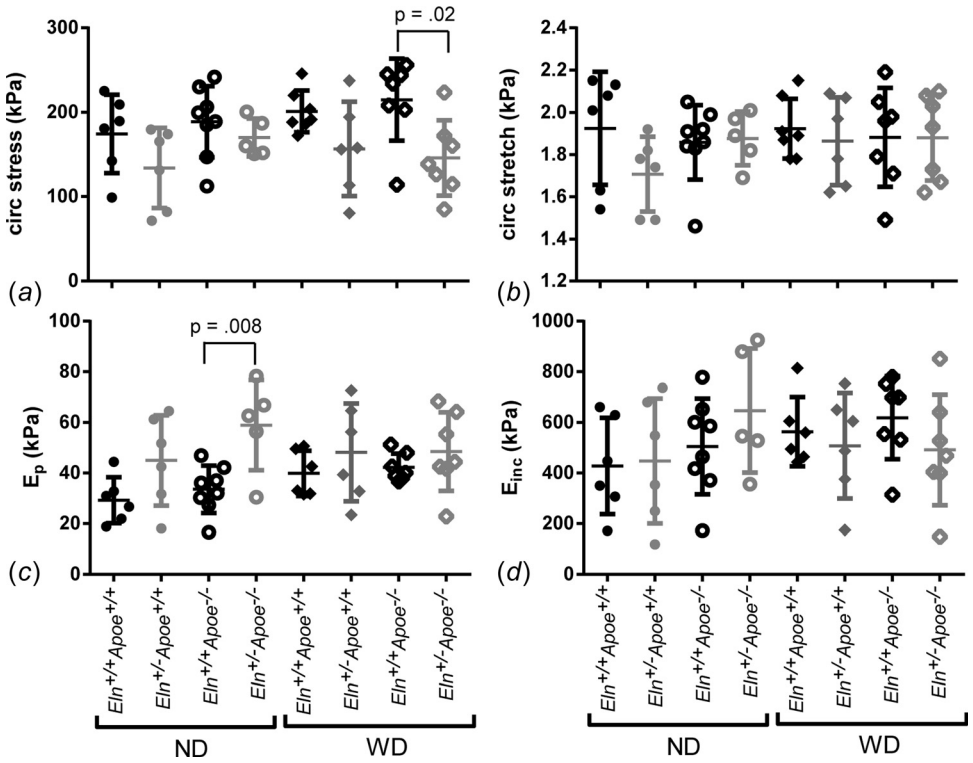

Fig. 4 Physiologic values of the systolic circumferential Cauchy stress (*a*), systolic circumferential stretch (*b*), structural stiffness (E_p) (*c*), and material stiffness (E_{inc}) (*d*) for the carotid artery were calculated using the mechanical test data and measured blood pressures. *P* values are from one-way ANOVA for *Eln* genotype. Results for three-way ANOVA are given in the text. Overall, $Eln^{+/-}$ carotid arteries have smaller systolic circumferential Cauchy stresses and larger E_p than $Eln^{+/+}$. Individual measurements are shown with mean±SD.

Cauchy stress or stretch, E_p, or E_{inc}, and there are no interactions between independent variables. By one-way ANOVA, there are significant differences between $Eln^{+/-}Apoe^{-/-}$ WD and $Eln^{+/+}Apoe^{-/-}$ WD for systolic circumferential Cauchy stress (Fig. 4(*a*)) and $Eln^{+/-}Apoe^{-/-}$ ND and $Eln^{+/+}Apoe^{-/-}$ ND for E_p (Fig. 4(*c*)). The differences in circumferential Cauchy stress highlight the importance of comparing physiologic values in addition to stress-stretch behavior. The differences in structural, but not material stiffnesses, are consistent with coordinated changes in unloaded dimensions and loaded pressure-diameter behavior for $Eln^{+/-}$ arteries.

Carotid Artery Wall Composition and Structure. To relate the observed changes in mechanical behavior to changes in composition of the arterial wall, we stained sections of the carotid artery for elastic VVG and collagen PSR fibers. Representative sections from mice on WD are shown in Fig. 5. Arterial sections for mice on ND are similar. $Eln^{+/-}$ arteries have an increased number of thinner elastic laminae across the wall, but there are no obvious breaks in or fragmentation of the elastic laminae, as shown previously [13,14]. In $Eln^{+/+}$ arteries, collagen fibers clearly outline each elastic laminae. In $Eln^{+/-}$ arteries, however, the collagen staining is more diffuse across the laminae thickness. The previous biochemical measurements showed that $Eln^{+/-}$ carotid arteries have 67% of the $Eln^{+/+}$ elastin amounts, with no change in total collagen amounts [11]. There are no apparent differences in wall composition between $Apoe^{+/+}$ and $Apoe^{-/-}$ arteries, supporting the limited differences in mechanical behavior observed as a result of *Apoe* genotype.

Atherosclerotic Plaque at the Aortic Root is Decreased, but Plaque in the Ascending Aorta is Increased in $Eln^{+/-}$ Mice. We compared plaque amounts from aortic root sections for each group after 12 weeks of ND or WD to determine the effects of increased structural stiffness in $Eln^{+/-}$ arteries on atherosclerotic plaque amounts. There are almost no detectable plaques at the aortic root for mice on ND or for $Apoe^{+/+}$ mice (Fig. 6). By three-way ANOVA, *Eln* genotype has no significant effect on plaque amounts at the aortic root, while *Apoe* genotype and WD increase plaque amounts by 6- and 20-fold, respectively ($p < 0.001$ for both). There are significant interactions between *Apoe* genotype and diet, as expected. When each individual group is compared using a one-way ANOVA for *Eln* genotype, there is a 105% decrease in aortic root plaque amounts in $Eln^{+/-}Apoe^{-/-}$ WD compared to $Eln^{+/+}Apoe^{-/-}$ WD.

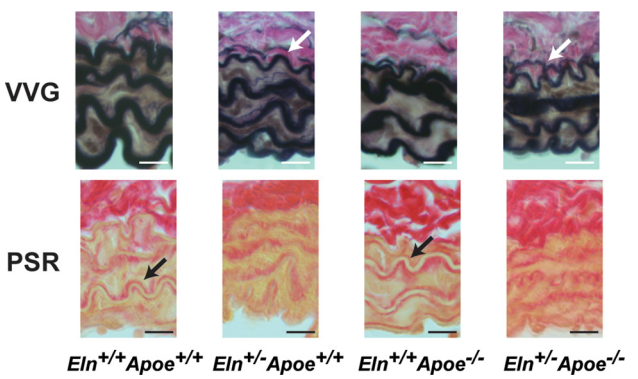

Fig. 5 Representative carotid artery sections stained with VVG (top) and PSR (bottom) for groups on WD. VVG stains elastic fibers black, muscle brown, and collagen pink. PSR stains collagen red on a pale yellow background. (Please refer to online article for color figures.) Note the additional layer of elastic fibers in $Eln^{+/-}$ VVG images (white arrows) and the clear outline of collagen fibers around the elastic fibers in $Eln^{+/+}$ PSR images (black arrows). Scale bars = 10 μm.

We also compared the percentage of the ascending aortic lumen area covered in plaque from en face preparations. Only 1% of the ascending aortic area has plaque in $Eln^{+/+}Apoe^{-/-}$ mice on ND; however, 8% of the ascending aortic area has plaque in $Eln^{+/-}Apoe^{-/-}$ mice on ND (Fig. 7). After 12 weeks on WD, both $Eln^{+/-}Apoe^{-/-}$ and $Eln^{+/+}Apoe^{-/-}$ mice have 18% of the ascending aortic area covered in plaque. In the ascending aorta, $Eln^{+/-}$ mice have 45% more plaque overall than $Eln^{+/+}$ ($p = 0.006$); $Apoe^{-/-}$ mice have 485% more plaque overall than $Apoe^{+/+}$ ($p < 0.001$), and mice on WD have 191% more plaque overall than mice on ND ($p < 0.001$) by three-way ANOVA. There are interactions between *Eln* and *Apoe* genotype ($p = 0.024$), *Eln* genotype and diet ($p = 0.004$), and *Apoe* genotype and diet ($p < 0.001$). When each individual group is compared for *Eln* genotype using a one-way ANOVA, there is a 581% increase in ascending aortic plaque area in $Eln^{+/-}Apoe^{-/-}$ ND mice compared to $Eln^{+/+}Apoe^{-/-}$ ND.

Our results indicate that increased structural stiffness in $Eln^{+/-}$ arteries modulates plaque amounts in $Apoe^{-/-}$ mice in a vascular location specific and diet-dependent manner. Since $Apoe^{-/-}$ mice on ND represent an earlier stage of atherosclerotic disease than $Apoe^{-/-}$ mice on WD [7], it is possible that $Eln^{+/-}$ mice have an altered disease progression compared to $Eln^{+/+}$ mice.

Alterations in Plaque Amounts are Not Due to Differences in Serum Cholesterol Levels in $Eln^{+/-}$ Mice. To see if altered cholesterol levels due to elastin haploinsufficiency may cause some of the changes in plaque amounts between groups, we measured serum levels of total cholesterol, triglyceride, LDL, and high density lipoprotein (HDL) levels. *Eln* genotype does not have a significant effect on any measures of cholesterol. $Apoe^{-/-}$ mice have six-fold more total cholesterol, three-fold more triglycerides, 36-fold more LDL, and 2.5-fold less HDL than $Apoe^{+/+}$ mice (Table 2). WD causes a 1.5-fold increase in total cholesterol and a 7.6-fold increase in LDL compared to ND. There are interactions between *Apoe* genotype and diet for total cholesterol, LDL, and HDL. $Apoe^{-/-}$ mice on WD have the expected cholesterol profiles and $Eln^{+/-}$ mice do not have any changes in cholesterol that may account for the differences in atherosclerotic plaque amounts.

Altered Plaque Amounts in $Eln^{+/-}Apoe^{-/-}$ Mice May be Linked to Serum Level Changes in Interleukin-6 or Transforming Growth Factor Beta 1. We further focused on $Apoe^{-/-}$ mice to investigate biochemical mechanisms for modulation of atherosclerotic plaque amounts by elastin haploinsufficiency. A multiplex panel of inflammatory cytokines was used, but only interleukin-6 (IL6), interleukin 10 (IL10), chemokine (C-X-C motif) ligand 1 (CXCL1), and tumor necrosis factor (TNF) were present in detectable levels in the mouse serum. The proinflammatory cytokines [23], CXCL1 and TNF, are increased 290% and 120%, respectively, with WD, and are not affected by *Eln* genotype (Table 3). Levels of IL10 are not affected by diet or *Eln* genotype. Levels of IL6 are increased 120% with WD and 120% with *Eln* genotype. TGF-β1 levels were also measured in $Apoe^{-/-}$ mice, as TGF-β1 is known to play a role in atherosclerosis formation [24]. Serum levels of TGF-β1 are decreased by 34% with *Eln* genotype and are not affected by diet. There are no interactions between diet and *Eln* genotype for any of the serum cytokine levels. Increases in IL6 and decreases in TGF-β1 may alter atherosclerosis progression in $Eln^{+/-}Apoe^{-/-}$ mice.

Discussion

Our results support those of Cilla et al. [9] that show no differences in structural or material stiffness between $Apoe^{-/-}$ and $Apoe^{+/+}$ arteries in young adult mice on ND. Cilla et al. [9] tested the entire aorta in situ, while we tested the left common carotid artery in vitro, demonstrating that similar results can be obtained for different testing methods and artery segments. Differences between our results and those of Agianniotis and Stergiopulos [8], who found that $Apoe^{-/-}$ thoracic aorta has increased stiffness, may be due to differences in vascular tone or to the higher axial stretch ratios (1.6–2.0) used in their study. We performed our experiments in the passive state, with no attempt to modulate arterial tone, while they performed experiments with fully activated or relaxed smooth muscle cells [8]. Huang et al. [25] found the global aortic stretch ratio of mouse aorta to be 1.4. Wagenseil et al. [12] showed that the pressure-diameter behavior of mouse arteries is insensitive to changes in axial stretch at or below the

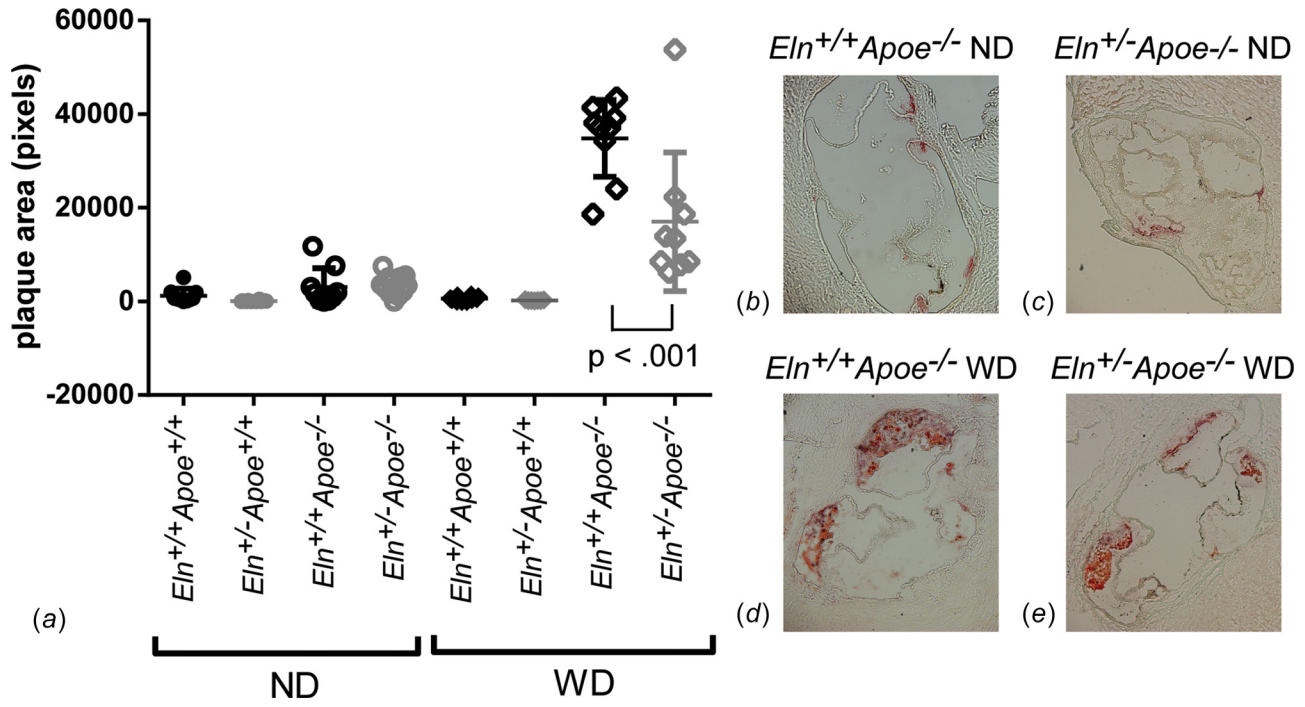

Fig. 6 Quantification of total plaque area at the aortic root (*a*). *P* value is from one-way ANOVA for *Eln* genotype. Results for three-way ANOVA are given in the text. Individual measurements are shown with mean±SD. Representative images of $Apoe^{-/-}$ aortic root sections stained with oil red O are shown in panels (*b*)–(*e*).

in vivo value, but sensitive to changes above the in vivo value. $Apoe^{-/-}$ aorta may be more sensitive to changes in the axial stretch ratio than $Apoe^{+/+}$. Bersi et al. [26] recently quantified passive in vitro biaxial mechanical behavior of different arterial segments of $Apoe^{-/-}$ mice. Although not directly compared to $Apoe^{+/+}$ arteries, the mechanical parameters calculated at systolic pressure, including circumferential and axial Cauchy stresses and material stiffnesses, appear similar to the mechanical parameters calculated for wild-type arteries in a different study by the same laboratory [27].

Crossing $Apoe^{-/-}$ with $Eln^{+/-}$ mice increases the structural arterial stiffness and allows investigation into the role of arterial stiffness in atherosclerotic disease. The increases in structural arterial stiffness for $Eln^{+/-}$ compared to $Eln^{+/+}$ mice are consistent with the changes associated with increased atherosclerosis in humans [28]. Despite the association between increased arterial stiffness and atherosclerosis in humans, we found that atherosclerotic plaque amounts in $Eln^{+/-}Apoe^{-/-}$ mice at the aortic valve were lower than and in the ascending aorta were similar to $Eln^{+/+}Apoe^{-/-}$ mice after 12 weeks on WD. However, we found that plaque amounts in the ascending aorta were significantly increased in $Eln^{+/-}Apoe^{-/-}$ mice compared to $Eln^{+/+}Apoe^{-/-}$ mice after 12 weeks on ND, suggesting that elastin haploinsufficiency alters atherosclerosis progression.

Our results confirm and extend the previous studies where we found that $Eln^{+/-}$ mice crossed with $Ldlr^{-/-}$ mice had similar or reduced amounts of plaque in the aortic valve and ascending aorta after 16 weeks on WD [13]. The time course of plaque development and the response to ND and WD are different in $Ldlr^{-/-}$ and $Apoe^{-/-}$ mice. Our two studies were designed so that we could achieve approximately equivalent atherosclerotic lesions in $Ldlr^{-/-}$ and $Apoe^{-/-}$ mice on WD (stage 3 [7]). Consequently, the mice on ND were at very different stages of lesion formation, with $Ldlr^{-/-}$ mice having no lesions and $Apoe^{-/-}$ mice having lesions between stages 1 and 2. Based on the plaque increase in $Eln^{+/-}$ $Apoe^{-/-}$ ascending aorta on ND, but not WD, we propose that increased structural arterial stiffness in $Eln^{+/-}$ mice accelerates atherosclerotic plaque accumulation in mice.

The previous animal studies have shown increased atherosclerotic plaques in models with increased arterial stiffness, but they have not focused on early stages of atherosclerosis and many of the models have alternative explanations for the differences in disease progression. For example, chronic infusion of angiotensin II (Ang II) in $Apoe^{-/-}$ mice on ND leads to increased systolic blood pressure, increased aortic stiffness, and increased plaque area compared to vehicle treated mice [29]. Ang II promotes apoptosis, fibrosis, and inflammation [30], all of which may contribute to increased plaque area. Increased arterial stiffness in mice with a mutation in the fibrillin-1 gene ($C1039G^{+/-}$) crossed into the $Apoe^{-/-}$ background and fed WD leads to higher plaque amounts at the aortic root and increased plaque instability compared to $C1039G^{+/+}Apoe^{-/-}$ mice [31]. Plaque rupture in $C1039G^{+/-}$ $Apoe^{-/-}$ mice on WD is attributed to elastic fiber fragmentation which causes the increase in arterial stiffness [32]. $C1039G^{+/-}$ mice also have alterations in TGF-β signaling [33] that may affect atherosclerosis progression [24]. Treating $Apoe^{-/-}$ mice on WD with a collagen crosslink inhibitor, beta-aminopropionitrile, decreases arterial stiffness and decreases atherosclerotic plaque area [34]. However, preventing crosslinking of collagen during plaque formation may limit the support matrix necessary for plaque accumulation.

Our study also offers several alternative explanations for the increased plaque amounts in $Eln^{+/-}Apoe^{-/-}$ mice on ND, besides increased structural arterial stiffness. One alternative explanation is increased blood pressure. Increased blood pressure may be caused by increased arterial stiffness [35] or by other mechanisms such as increased peripheral resistance and activation of the renin-angiotensin pathway [36]. $Eln^{+/-}$ mice have alterations in

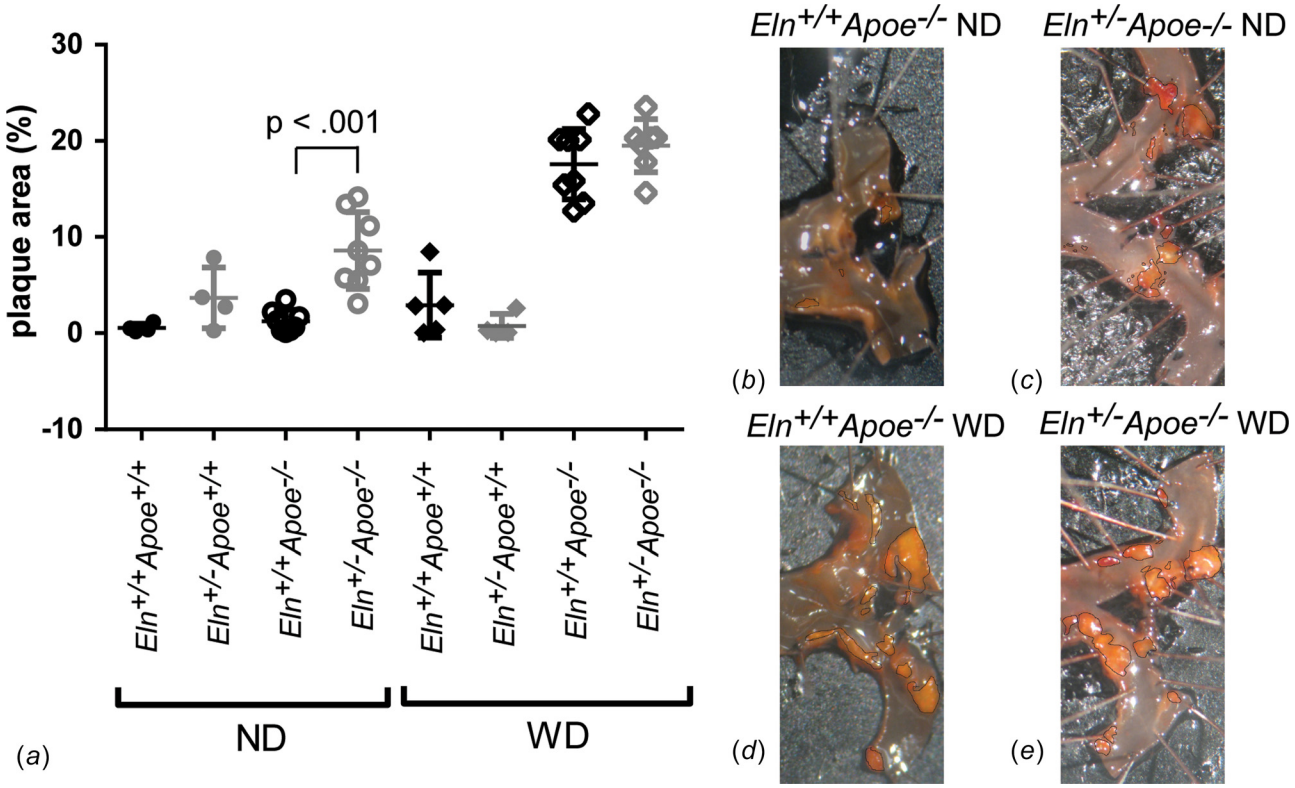

Fig. 7 Quantification of the percentage of the ascending aorta lumen area covered in plaque (*a*). *P* value is from one-way ANOVA for *Eln* genotype. Results for three-way ANOVA are given in the text. Individual measurements are shown with mean±SD. Representative images of $Apoe^{-/-}$ ascending aorta en face preparations stained with oil red O are shown in panels (*b*)–(*e*).

resistance vessel structure and contractility [37] and increased renin levels [11] that may contribute to changes in blood pressure and atherosclerosis progression. Additionally, we found that TGF-β1 levels in $Eln^{+/+}Apoe^{-/-}$ mice are similar to those measured in wild-type mice [38], but are reduced in $Eln^{+/-}Apoe^{-/-}$ mice. The previous animal studies have shown relationships between decreased TGF-β levels and accelerated atherosclerosis [24]. In humans, circulating active TGF-β levels are negatively correlated with coronary atherosclerosis [39].

The development and progression of atherosclerosis depend on signaling of inflammatory molecules. IL6, CXCL1, and TNF are proinflammatory molecules [23] that are upregulated with WD and the resulting increased amounts of atherosclerotic plaque. IL6 is also upregulated in $Eln^{+/-}Apoe^{-/-}$ mice, independent of diet. Increased IL6 may be a cause or consequence of the acceleration of plaque accumulation in $Eln^{+/-}Apoe^{-/-}$ mice. IL6 levels in humans positively correlate with coronary atherosclerosis [39]. IL6 expression is differentially regulated by cyclic stretch in vascular smooth muscle and endothelial cells [40], so increased arterial stiffness may lead to alterations in IL6 signaling. There is extensive crosstalk between TGF-β and IL6 signaling [41], so altered TGF-β1 levels in $Eln^{+/-}Apoe^{-/-}$ mice may also lead to changes in IL6 levels. TGF-β can have anti- or proinflammatory effects depending on the cellular context and presence of other signaling molecules [42]. Additional work is needed to understand how changes in circulating cytokines could mediate atherosclerotic plaque amounts in $Eln^{+/-}Apoe^{-/-}$ mice.

Regardless of the molecular mechanisms leading to increased plaque amounts at early stages of atherosclerotic disease, we saw reduced or similar amounts of plaque at later disease stages in $Eln^{+/-}Apoe^{-/-}$ mice. At the aortic valve, there is a decrease in plaque amounts in $Eln^{+/-}Apoe^{-/-}$ mice compared to $Eln^{+/+}Apoe^{-/-}$ on WD. There is also a reduction in carotid artery circumferential Cauchy stress in $Eln^{+/-}Apoe^{-/-}$ mice compared to $Eln^{+/+}Apoe^{-/-}$ on WD, mostly due to the reduction in systolic inner diameter. The systolic inner diameter of the carotid artery is 20% smaller in mice with $Eln^{+/-}$ genotype compared to $Eln^{+/+}$ in the current study (not shown), which is comparable to results for the ascending aortic diameter at systole in $Eln^{+/-}$ compared to $Eln^{+/+}$ mice from in vivo ultrasound studies [43]. For similar cardiac output values [43], the mean wall shear stress scales with the $1/\text{radius}^3$, so a 20% decrease in radius would lead to a 95% increase in mean wall shear stress. Higher wall shear stresses may be protective [44] against large amounts of atherosclerotic plaque build-up at the $Eln^{+/-}$ aortic root. However, the ascending aorta was not protected from plaque formation in $Eln^{+/-}Apoe^{-/-}$ compared to $Eln^{+/+}Apoe^{-/-}$ mice on WD. Shear stress depends on many factors besides inner diameter, including arterial curvature and branching pattern, and blood flow rate and waveform shape [45]. The curvature and branching angles are altered in $Eln^{+/-}$ arteries [43], and the blood flow rate and waveform shape are affected by increased arterial stiffness. Computational models and detailed experimental measurements are necessary to calculate wall shear stress at different locations and determine whether local shear stress is increased or decreased in $Eln^{+/-}$ arteries.

Our results show that elastin haploinsufficiency increases plaque amounts at early stages of atherosclerotic disease, but does not increase plaque amounts at later disease stages. $Eln^{+/-}Apoe^{-/-}$ mice have changes in structural stiffness and circumferential Cauchy stress in the carotid artery, increased blood pressure, and alterations in circulating IL6 and TGF-β1 levels, that lead to increased plaque amounts in the ascending aorta compared to $Eln^{+/+}Apoe^{-/-}$ mice on ND, but no increases in plaque amounts in the ascending aorta on WD. It is likely that the effects of altered arterial mechanics, blood pressure, and circulating cytokine levels cannot be completely separated, but it is possible that modulating one or several factors may alter atherosclerotic disease progression. Modulating arterial mechanics, blood pressure, and/or circulating cytokine levels will be important for managing atherosclerotic disease in humans with elastin haploinsufficiency [14], essential hypertension [46], increased arterial stiffness in aging [1], and extracellular matrix defects that modulate TGF-β availability [47].

Limitations and Future Directions. Limitations of the current study include the use of mouse models that do not precisely mimic human atherosclerotic disease, the relatively short disease progression investigated at a single time point, and the lack of characterization of plaque composition. There are likely differences in atherosclerotic plaque progression, such as macrophage type and localization and fibrous cap thickness, that depend on elastin haploinsufficiency and were not captured in our gross examination of plaque amounts. Future studies with more detailed plaque composition analyses, macrophage phenotypes, and a time course of disease progression could identify subtle differences between genotypes. More detailed plaque analyses may also help identify the cellular source of the alterations in circulating IL6 and TGF-β1. We measured arterial stiffness in the carotid artery, but atherosclerotic plaque amounts at the aortic root and in the ascending aorta. The previous work has shown consistent changes in arterial mechanical behavior due to elastin haploinsufficiency in mice [11,12], but additional mechanical measurements could be performed at the plaque sites. In our previous study with $Eln^{+/-}Ldlr^{-/-}$ mice, we measured arterial stiffness and plaque amounts in the ascending aorta and found similar trends to the current study for mice on WD [13]. We propose that increased structural arterial stiffness is a factor that accelerates atherosclerotic plaque accumulation in $Eln^{+/-}Apoe^{-/-}$ mice. Our hypothesis could be further investigated using other genetic mouse models with increased arterial stiffness.

Acknowledgment

Trey Coleman at the Washington University School of Medicine is gratefully acknowledged for providing assistance with the plaque quantification methods. The Immunomonitoring Laboratory in the Center for Human Immunology and Immunotherapy Programs at Washington University performed the immunoassays.

Funding Data

- NIH R01HL105314 (JEW).
- NIH R01HL115560 (JEW).
- American Diabetes Association grant 7-13-JF-16 (CSC).
- Washington University Nutrition and Obesity Research Center grant P30DK056341 (CSC).
- NIH P30DK052574 (DDRCC).

Nomenclature

Apoe = Apolipoprotein E
CXCL1 = chemokine (C-X-C motif) ligand 1
Eln = elastin
E_{inc} = incremental Young's modulus
E_p = Peterson's modulus
H&E = hematoxylin and eosin
HDL = high density lipoprotein
IL6 = interleukin-6
IL10 = interleukin-10
LDL = low density lipoprotein
ND = normal diet
PSR = picrosirius red
PWV = pulse wave velocity
TGF-β1 = transforming growth factor beta 1
TNF = tumor necrosis factor
VVG = Verhoeff Van Gieson
WD = western diet

References

[1] Yamashina, A., Tomiyama, H., Arai, T., Hirose, K., Koji, Y., Hirayama, Y., Yamamoto, Y., and Hori, S., 2003, "Brachial-Ankle Pulse Wave Velocity as a Marker of Atherosclerotic Vascular Damage and Cardiovascular Risk," Hypertens. Res., **26**(8), pp. 615–622.

[2] Gosling, R. G., and Budge, M. M., 2003, "Terminology for Describing the Elastic Behavior of Arteries," Hypertension, **41**(6), pp. 1180–1182.

[3] Palombo, C., and Kozakova, M., 2016, "Arterial Stiffness, Atherosclerosis and Cardiovascular Risk: Pathophysiologic Mechanisms and Emerging Clinical Indications," Vasc. Pharmacol., **77**, pp. 1–7.

[4] Birukov, K. G., 2009, "Cyclic Stretch, Reactive Oxygen Species, and Vascular Remodeling," Antioxid. Redox Signal, **11**(7), pp. 1651–1667.

[5] Isenberg, B. C., Dimilla, P. A., Walker, M., Kim, S., and Wong, J. Y., 2009, "Vascular Smooth Muscle Cell Durotaxis Depends on Substrate Stiffness Gradient Strength," Biophys J., **97**(5), pp. 1313–1322.

[6] Zhang, S. H., Reddick, R. L., Piedrahita, J. A., and Maeda, N., 1992, "Spontaneous Hypercholesterolemia and Arterial Lesions in Mice Lacking Apolipoprotein E," Science, **258**(5081), pp. 468–471.

[7] Whitman, S. C., 2004, "A Practical Approach to Using Mice in Atherosclerosis Research," Clin. Biochem. Rev., **25**(1), pp. 81–93.

[8] Agianniotis, A., and Stergiopulos, N., 2012, "Wall Properties of the Apolipoprotein E-Deficient Mouse Aorta," Atherosclerosis, **223**(2), pp. 314–320.

[9] Cilla, M., Perez, M. M., Pena, E., and Martinez, M. A., 2016, "Effect of Diet and Age on Arterial Stiffening Due to Atherosclerosis in ApoE(-/-) Mice," Ann. Biomed. Eng., **44**(7), pp. 2202–2217.

[10] Cheng, C., Tempel, D., van Haperen, R., van der Baan, A., Grosveld, F., Daemen, M. J., Krams, R., and de Crom, R., 2006, "Atherosclerotic Lesion Size and Vulnerability Are Determined by Patterns of Fluid Shear Stress," Circulation, **113**(23), pp. 2744–2753.

[11] Faury, G., Pezet, M., Knutsen, R. H., Boyle, W. A., Heximer, S. P., McLean, S. E., Minkes, R. K., Blumer, K. J., Kovacs, A., Kelly, D. P., Li, D. Y., Starcher, B., and Mecham, R. P., 2003, "Developmental Adaptation of the Mouse Cardiovascular System to Elastin Haploinsufficiency," J. Clin Invest., **112**(9), pp. 1419–1428.

[12] Wagenseil, J. E., Nerurkar, N. L., Knutsen, R. H., Okamoto, R. J., Li, D. Y., and Mecham, R. P., 2005, "Effects of Elastin Haploinsufficiency on the Mechanical Behavior of Mouse Arteries," Am. J. Physiol. Heart. Circ. Physiol., **289**(3), pp. H1209–H1217.

[13] Maedeker, J. A., Stoka, K. V., Bhayani, S. A., Gardner, W. S., Bennett, L., Procknow, J. D., Staiculescu, M. C., Walji, T. A., Craft, C. S., and Wagenseil, J. E., 2016, "Hypertension and Decreased Aortic Compliance Due to Reduced Elastin Amounts Do Not Increase Atherosclerotic Plaque Accumulation in Ldlr-/- Mice," Atherosclerosis, **249**, pp. 22–29.

[14] Li, D. Y., Faury, G., Taylor, D. G., Davis, E. C., Boyle, W. A., Mecham, R. P., Stenzel, P., Boak, B., and Keating, M. T., 1998, "Novel Arterial Pathology in Mice and Humans Hemizygous for Elastin," J. Clin. Invest., **102**(10), pp. 1783–1787.

[15] Amin, M., Kunkel, A. G., Le, V. P., and Wagenseil, J. E., 2011, "Effect of Storage Duration on the Mechanical Behavior of Mouse Carotid Artery," ASME J. Biomech. Eng., **133**(7), p. 071007.

[16] Dobrin, P. B., 1996, "Effect of Histologic Preparation on the Cross-Sectional Area of Arterial Rings," J. Surg. Res., **61**(2), pp. 413–415.

[17] Humphrey, J. D., 2002, *Cardiovascular Solid Mechanics*, Springer-Verlag, New York.

[18] Fonck, E., Prod'hom, G., Roy, S., Augsburger, L., Rufenacht, D. A., and Stergiopulos, N., 2007, "Effect of Elastin Degradation on Carotid Wall Mechanics as Assessed by a Constituent-Based Biomechanical Model," Am. J. Physiol. Heart Circ. Physiol., **292**(6), pp. H2754–H2763.

[19] Semenkovich, C. F., Coleman, T., and Daugherty, A., 1998, "Effects of Heterozygous Lipoprotein Lipase Deficiency on Diet-Induced Atherosclerosis in Mice," J. Lipid Res., **39**(6), pp. 1141–1151.

[20] Tangirala, R. K., Rubin, E. M., and Palinski, W., 1995, "Quantitation of Atherosclerosis in Murine Models: Correlation Between Lesions in the Aortic Origin and in the Entire Aorta, and Differences in the Extent of Lesions Between Sexes in LDL Receptor-Deficient and Apolipoprotein E-Deficient Mice," J. Lipid Res., **36**(11), pp. 2320–2328.

[21] Ghasemi, A., and Zahediasl, S., 2012, "Normality Tests for Statistical Analysis: A Guide for Non-Statisticians," Int. J. Endocrinol. Metab., **10**(2), pp. 486–489.

[22] Harwell, M. R., Rubinstein, E. N., Hayes, W. S., and Olds, C. C., 1992, "Summarizing Monte Carlo Results in Methodological Research - the 1-Factor and 2-Factor Fixed Effects Anova Cases," J. Educ. Stat., **17**(4), pp. 315–339.

[23] Turner, M. D., Nedjai, B., Hurst, T., and Pennington, D. J., 2014, "Cytokines and Chemokines: At the Crossroads of Cell Signalling and Inflammatory Disease," Biochim. Biophys. Acta, **1843**(11), pp. 2563–2582.

[24] Mallat, Z., Gojova, A., Marchiol-Fournigault, C., Esposito, B., Kamate, C., Merval, R., Fradelizi, D., and Tedgui, A., 2001, "Inhibition of Transforming Growth Factor-Beta Signaling Accelerates Atherosclerosis and Induces an Unstable Plaque Phenotype in Mice," Circ. Res., **89**(10), pp. 930–934.

[25] Huang, Y., Guo, X., and Kassab, G. S., 2006, "Axial Nonuniformity of Geometric and Mechanical Properties of Mouse Aorta is Increased During Postnatal Growth," Am. J. Physiol. Heart Circ. Physiol., **290**(2), pp. H657–H664.

[26] Bersi, M. R., Khosravi, R., Wujciak, A. J., Harrison, D. G., and Humphrey, J. D., 2017, "Differential Cell-Matrix Mechanoadaptations and Inflammation Drive Regional Propensities to Aortic Fibrosis, Aneurysm or Dissection in Hypertension," J. R. Soc. Interface, **14**(136), p. 20170327.

[27] Ferruzzi, J., Bersi, M. R., Uman, S., Yanagisawa, H., and Humphrey, J. D., 2015, "Decreased Elastic Energy Storage, Not Increased Material Stiffness, Characterizes Central Artery Dysfunction in Fibulin-5 Deficiency Independent of Sex," ASME J. Biomech. Eng., **137**(3), p. 031007.

[28] van Popele, N. M., Grobbee, D. E., Bots, M. L., Asmar, R., Topouchian, J., Reneman, R. S., Hoeks, A. P., van der Kuip, D. A., Hofman, A., and Witteman, J. C., 2001, "Association Between Arterial Stiffness and Atherosclerosis: The Rotterdam Study," Stroke, **32**(2), pp. 454–460.

[29] Tham, D. M., Martin-McNulty, B., Wang, Y. X., Da Cunha, V., Wilson, D. W., Athanassious, C. N., Powers, A. F., Sullivan, M. E., and Rutledge, J. C., 2002, "Angiotensin II Injures the Arterial Wall Causing Increased Aortic Stiffening in Apolipoprotein E-Deficient Mice," Am. J. Physiol. Regul. Integr. Comp. Physiol., **283**(6), pp. R1442–R1449.

[30] van Thiel, B. S., van der Pluijm, I., Te Riet, L., Essers, J., and Danser, A. H., 2015, "The Renin-Angiotensin System and Its Involvement in Vascular Disease," Eur. J. Pharmacol., **763**(Pt. A), pp. 3–14.

[31] Van Herck, J. L., De Meyer, G. R., Martinet, W., Van Hove, C. E., Foubert, K., Theunis, M. H., Apers, S., Bult, H., Vrints, C. J., and Herman, A. G., 2009, "Impaired Fibrillin-1 Function Promotes Features of Plaque Instability in Apolipoprotein E-Deficient Mice," Circulation, **120**(24), pp. 2478–2487.

[32] Van der Donckt, C., Van Herck, J. L., Schrijvers, D. M., Vanhoutte, G., Verhoye, M., Blockx, I., Van Der Linden, A., Bauters, D., Lijnen, H. R., Sluimer, J. C., Roth, L., Van Hove, C. E., Fransen, P., Knaapen, M. W., Hervent, A. S., De Keulenaer, G. W., Bult, H., Martinet, W., Herman, A. G., and De Meyer, G. R., 2015, "Elastin Fragmentation in Atherosclerotic Mice Leads to Intraplaque Neovascularization, Plaque Rupture, Myocardial Infarction, Stroke, and Sudden Death," Eur. Heart J., **36**(17), pp. 1049–1058.

[33] Habashi, J. P., Judge, D. P., Holm, T. M., Cohn, R. D., Loeys, B. L., Cooper, T. K., Myers, L., Klein, E. C., Liu, G., Calvi, C., Podowski, M., Neptune, E. R., Halushka, M. K., Bedja, D., Gabrielson, K., Rifkin, D. B., Carta, L., Ramirez, F., Huso, D. L., and Dietz, H. C., 2006, "Losartan, an AT1 Antagonist, Prevents Aortic Aneurysm in a Mouse Model of Marfan Syndrome," Science, **312**(5770), pp. 117–121.

[34] Kothapalli, D., Liu, S. L., Bae, Y. H., Monslow, J., Xu, T., Hawthorne, E. A., Byfield, F. J., Castagnino, P., Rao, S., Rader, D. J., Pure, E., Phillips, M. C., Lund-Katz, S., Janmey, P. A., and Assoian, R. K., 2012, "Cardiovascular Protection by ApoE and ApoE-HDL Linked to Suppression of ECM Gene Expression and Arterial Stiffening," Cell Rep., **2**(5), pp. 1259–1271.

[35] Kaess, B. M., Rong, J., Larson, M. G., Hamburg, N. M., Vita, J. A., Levy, D., Benjamin, E. J., Vasan, R. S., and Mitchell, G. F., 2012, "Aortic Stiffness, Blood Pressure Progression, and Incident Hypertension," JAMA, **308**(9), pp. 875–881.

[36] Mayet, J., and Hughes, A., 2003, "Cardiac and Vascular Pathophysiology in Hypertension," Heart, **89**(9), pp. 1104–1109.

[37] Osei-Owusu, P., Knutsen, R. H., Kozel, B. A., Dietrich, H. H., Blumer, K. J., and Mecham, R. P., 2014, "Altered Reactivity of Resistance Vasculature Contributes to Hypertension in Elastin Insufficiency," Am. J. Physiol. Heart Circ. Physiol., **306**(5), pp. H654–H666.

[38] Matt, P., Schoenhoff, F., Habashi, J., Holm, T., Van Erp, C., Loch, D., Carlson, O. D., Griswold, B. F., Fu, Q., De Backer, J., Loeys, B., Huso, D. L., McDonnell, N. B., Van Eyk, J. E., Dietz, H. C., and The GenTAC Consortium, 2009, "Circulating Transforming Growth Factor-β in Marfan Syndrome," Circulation, **120**(6), pp. 526–532.

[39] Erren, M., Reinecke, H., Junker, R., Fobker, M., Schulte, H., Schurek, J. O., Kropf, J., Kerber, S., Breithardt, G., Assmann, G., and Cullen, P., 1999, "Systemic Inflammatory Parameters in Patients With Atherosclerosis of the Coronary and Peripheral Arteries," Arterioscler., Thromb., Vasc. Biol., **19**(10), pp. 2355–2363.

[40] Anwar, M. A., Shalhoub, J., Lim, C. S., Gohel, M. S., and Davies, A. H., 2012, "The Effect of Pressure-Induced Mechanical Stretch on Vascular Wall Differential Gene Expression," J. Vasc. Res., **49**(6), pp. 463–478.

[41] Guo, X., and Wang, X. F., 2009, "Signaling Cross-Talk Between TGF-Beta/BMP and Other Pathways," Cell Res., **19**(1), pp. 71–88.

[42] Topper, J. N., 2000, "TGF-Beta in the Cardiovascular System: Molecular Mechanisms of a Context-Specific Growth Factor," Trends Cardiovasc. Med., **10**(3), pp. 132–137.

[43] Le, V. P., and Wagenseil, J. E., 2012, "Echocardiographic Characterization of Postnatal Development in Mice With Reduced Arterial Elasticity," Cardiovasc. Eng. Technol., **3**(4), pp. 424–438.

[44] Cunningham, K. S., and Gotlieb, A. I., 2005, "The Role of Shear Stress in the Pathogenesis of Atherosclerosis," Lab Invest., **85**(1), pp. 9–23.

[45] Myers, J. G., Moore, J. A., Ojha, M., Johnston, K. W., and Ethier, C. R., 2001, "Factors Influencing Blood Flow Patterns in the Human Right Coronary Artery," Ann. Biomed. Eng., **29**(2), pp. 109–120.

[46] Oyama, N., Gona, P., Salton, C. J., Chuang, M. L., Jhaveri, R. R., Blease, S. J., Manning, A. R., Lahiri, M., Botnar, R. M., Levy, D., Larson, M. G., O'Donnell, C. J., and Manning, W. J., 2008, "Differential Impact of Age, Sex, and Hypertension on Aortic Atherosclerosis: The Framingham Heart Study," Arterioscler., Thromb., Vasc. Biol., **28**(1), pp. 155–159.

[47] Robertson, I. B., and Rifkin, D. B., 2016, "Regulation of the Bioavailability of TGF-β and TGF-β-Related Proteins," Cold Spring Harbor Perspect. Biol., **8**(6), p. a021907.